

UNCLASSIFIED

AD NUMBER
AD893904
NEW LIMITATION CHANGE
TO Approved for public release, distribution unlimited
FROM Distribution authorized to U.S. Gov't. agencies only; Test and Evaluation; Apr 1972. Other requests shall be referred to Director, Naval Research Laboratory, Washington, DC 20390.
AUTHORITY
NRL ltr, 27 Jun 1983

THIS PAGE IS UNCLASSIFIED

✓

NRL Report 7407

Airborne Radar Motion Compensation Techniques
Evaluation of TACCAR

G. A. ANDREWS, JR.

*Airborne Radar Branch
Radar Division*

AD 8939 04

April 12, 1972



NAVAL RESEARCH LABORATORY
Washington, D.C.

Distribution limited to U.S. Government Agencies only; test and evaluation, April 1972. Other requests for this document must be referred to the Director, Naval Research Laboratory, Washington, D.C. 20390.

MEMORANDUM

Subject: Airborne Radar Motion Compensation Techniques, Evaluation of TACCAR

Background

As a part of the Airborne Tactical Control System (ATCS) program, the Airborne Radar Branch is developing AMTI techniques to increase the detectability of moving targets in clutter. Investigations are underway to determine the limitations of existing systems. Since good AMTI performance depends heavily on motion compensation, an analysis of motion compensation techniques was initiated.

Findings

The component of aircraft motion which is perpendicular to the antenna aperture causes unacceptable losses to AMTI performance for AEW applications. TACCAR only partially compensates for this motion and therefore will limit the capability of advanced AMTI systems. However, an extension of the TACCAR concept can reduce this limitation to a point well below other system limitations. This extension consists of making doppler corrections at more than the one point normally made by TACCAR.

Recommended Action

Advanced AMTI systems attempting to obtain high cancellation ratios should use multiple correction points. The number of correction points depends on the desired cancellation ratio. A complete developmental program should be conducted to determine (1) optimum implementation of such a system and (2) the effect of operating conditions on the phase-lock loop design for such a system.

R & D Implications

A thorough motion compensation philosophy using combined array/time processing should be developed to prevent advanced AMTI systems from being limited by platform motion.



G. A. Andrews
ATCS Section
AIRBORNE RADAR BRANCH

CONTENTS

Abstract	iii
Authorization	iii
Introduction	1
Description of TACCAR	1
TACCAR Range Error	2
Effect of Error on MTI	6
Reduction of TACCAR Loss	13
Conclusion	16
References	19
Appendices	
A - Derivation of MTI Improvement Factor	A1
B - Derivation of MTI Improvement Factor for Clutter with Non-zero Mean Spectrum	B1

Abstract

Coherent signal processing in many classes of airborne radar systems is limited by the methods used to compensate for platform motion. Platform motion causes doppler shifts of returns which vary with the angle between the velocity vector and the scatterer. Because of the finite antenna beamwidth and finite transmitted pulse length, the returns from many scatterers are received simultaneously. These returns have different doppler shifts which result in a spectrum of received doppler frequencies. This spectrum degrades the performance of radar systems that coherently process these returns.

Time Average Clutter Coherent Airborne Radar (TACCAR) is a widely used technique to compensate for the component of motion which is parallel to the axis of the beam. This report evaluates TACCAR in terms of its improvement to moving target indicator (MTI) performance. It is shown that MTI performance can be improved significantly with extensions to the TACCAR concept.

Authorization

NRL Problem 53R02-29
A360-5333/652B/2F00-141-601

Manuscript submitted February 16, 1972.

AIRBORNE RADAR MOTION COMPENSATION TECHNIQUES

EVALUATION OF TACCAR

Introduction

The application of digital processing techniques to airborne early warning radar systems has made it practical to coherently process many radar returns using multiple-stage MTI cancellers and coherent integration (narrow-band doppler filtering). The resulting clutter rejection capability improves the detection of moving targets in clutter to the point where limitations other than those imposed by these processing techniques prevent further system improvement.

Existing systems may be limited by factors such as system stability or on-aircraft antenna sidelobes. As these or other limitations are alleviated, the motion compensation techniques may become the limit to system performance.

It is in this context that Time Average Clutter Coherent Airborne Radar (TACCAR), which was originated by the MIT Lincoln Laboratory and has performed very successfully with past radar systems, is considered. TACCAR, which corrects for the component of platform velocity parallel to the axis of the antenna beam pattern, and Displaced Phase Center Array (DPCA), which was developed by the General Electric Company and which corrects for the perpendicular component of platform velocity, make up the motion compensation techniques which are being applied to present airborne early warning radar systems. An evaluation of DPCA will follow in another report.

The success of a motion compensation technique must be evaluated in terms of the improvement it provides to the signal processing in the radar receiver. Since many airborne radar systems now (and will in the foreseeable future) involve moving target indicator (MTI) processing, the improvement in MTI gain will be used to measure the performance of TACCAR.

Description of TACCAR

The assignment of the processor in an MTI radar is to discriminate between moving and stationary objects. Although for some radar applications, the returns from stationary objects are of interest, these returns are "clutter" in an MTI radar and must be rejected. The rejection decision is based upon the doppler shifts of the returns. If the radar is on a moving platform, the returns from stationary objects contain a doppler shift which must be removed to provide good MTI performance.

A detailed description of TACCAR may be found in Ref. 1. The detailed block diagram for TACCAR has many configurations in practice. In all cases, the processing takes the form of estimating the average doppler shift of the returns from all objects within the antenna pattern and within some sampling interval. This average doppler is removed by shifting either the transmitted or local oscillator frequency.

The technique that is common to the various configurations of TACCAR is a gated phase-lock loop which is used to correct for the average doppler shift during a selected interval of time as shown in the simplified block diagram in Fig. 1.

This widely used technique in coherent communications systems is thoroughly analyzed in Refs. 2, 3. For TACCAR, the phase-lock loop is gated on at some time interval corresponding to a selected range interval. The integrator and sample-and-hold network give an estimate of the average doppler during this range interval. This estimate is repeated during each repetition interval.

To fully evaluate the capability of TACCAR, the performance of this phase-lock loop as a function of the length of the sampling interval, the time constant of the integrator, and the variance of the signal spectrum must be considered. Analysis of the loop shows that a relatively long time constant (several pulse repetition intervals) is needed in the integrator for good loop performance and to maintain pulse-to-pulse coherency for MTI cancellation. Thus, a single loop can make only one correction for all ranges, and changes in doppler with range will not be corrected without additional processing. It is this error versus range that is addressed in this report.

TACCAR Range Errors

If an object is located at an angle, (θ_s, ϕ_s) , with respect to the aircraft velocity vector, v_p , it has an "apparent" velocity, $-v_p$ as shown in Fig. 2.

The "apparent" velocity of the object has a normal component,

$$v_n = -v_p \cos \theta_s \cos \phi_s$$
 and a tangential component,

$$v_t = -v_p \sin \theta_s \cos \phi_s$$

The doppler shift of a return from this object is approximately

$$f_d = -2 \frac{v_n}{c} f_t$$

where f_t is transmitted frequency
 c is propagation velocity

If the axis of the antenna pattern is pointing in a direction, (θ_a, ϕ_a) , with respect to the aircraft velocity vector, and if the object is at an angle, (θ, ϕ) , with respect to the axis of the antenna pattern,

$$\begin{aligned} \theta_s &= \theta_a + \theta, \text{ and} \\ \phi_s &= \phi_a + \phi \end{aligned}$$

So that:

$$v_n = -v_p \cos \phi_s \cos (\theta_a + \theta).$$

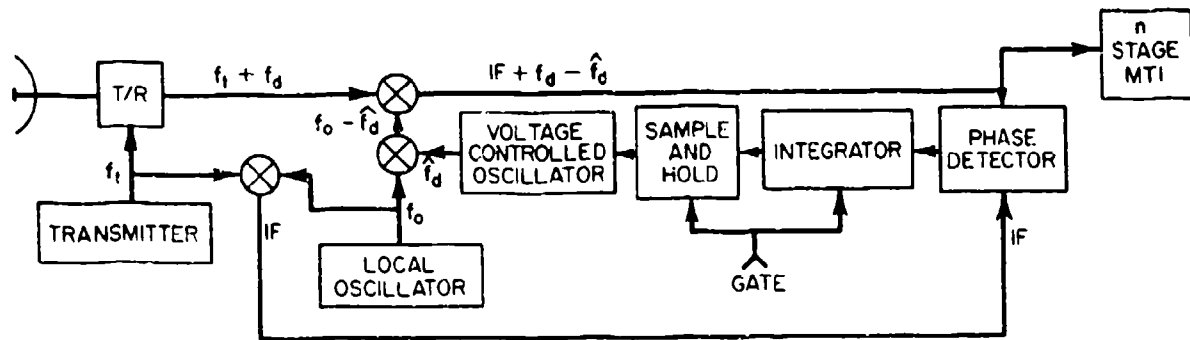


Fig. 1 - Simplified block diagram of TACCAR

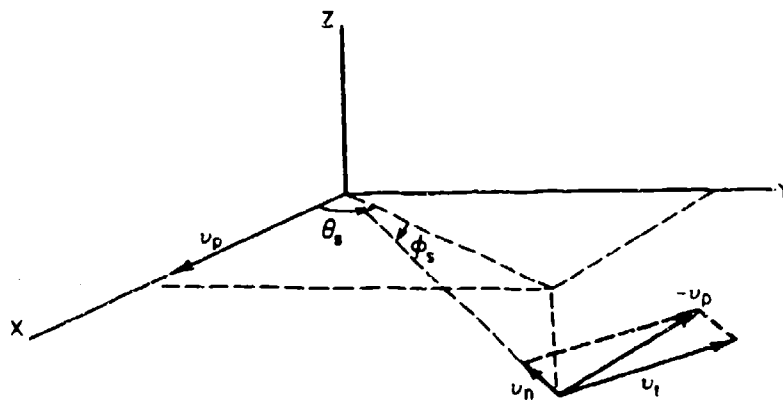


Fig. 2 - Velocity relationship's

Or

$$f_d = \frac{2 v_p}{\lambda} \cos \theta_s (\cos \theta_a \cos \theta - \sin \theta_a \sin \theta)$$

When f_d is averaged over a symmetrical antenna pattern,

$$\bar{f}_d = f_d \Big|_{\theta=0} = 2 \frac{v_p}{\lambda} \cos \theta_s \cos \theta_a$$

TACCAR estimates \bar{f}_d and subtracts it from f_d to give a corrected doppler of

$$\begin{aligned} f'_d &= f_d - \bar{f}_d \\ &= 2 \frac{v_p}{\lambda} \cos \theta_s \left[\cos \theta_a (\cos \theta - 1) - \sin \theta_a \sin \theta \right], \end{aligned}$$

if the estimate of \bar{f}_d is without error.

With the aircraft flying at an altitude, H, above the surface of the earth, the elevation angle, θ_s , of a scatterer on the surface is a function of H and the range, R_s , to the scatterer. This relationship is plotted in Ref. 1 (page 18-4, Fig. 4) and is reproduced in Fig. 3.

In the design of the usual TACCAR loop, a single range interval during which the loop will be gated on is selected. However, since Fig. 3 indicates that θ_s , and therefore f_d , is a function of range to the object, \bar{f}_d as developed from a single range interval will not develop the optimum correction at all ranges. The problem then is to select that range interval which will minimize peak error. To use this criterion, a maximum and a minimum range must be selected which, using Fig. 3, gives for $\cos \theta_s$ maximum ($\cos \theta_{\max}$) and minimum ($\cos \theta_{\min}$) values.

Minimization of the peak error implies estimating,

$$\begin{aligned} \hat{f}_d &= \frac{f_{d \max} + f_{d \min}}{2} \\ &= \frac{v_p \cos \theta_a}{\lambda} (\cos \theta_{\max} + \cos \theta_{\min}). \end{aligned}$$

Using this estimate, the absolute value of the error versus range (or $\cos \theta_s$) is:

$$|f_e| = \left| \frac{2 v_p \cos \theta_a}{\lambda} \left(\cos \theta_s - \frac{\cos \theta_{\max} + \cos \theta_{\min}}{2} \right) \right|$$

Normalizing:

$$e_n = \left| \frac{f_e}{(2v_p \cos \theta_a)/\lambda} \right| = \left| \left(\cos \theta_s - \frac{\cos \theta_{\max} + \cos \theta_{\min}}{2} \right) \right| \quad (1)$$

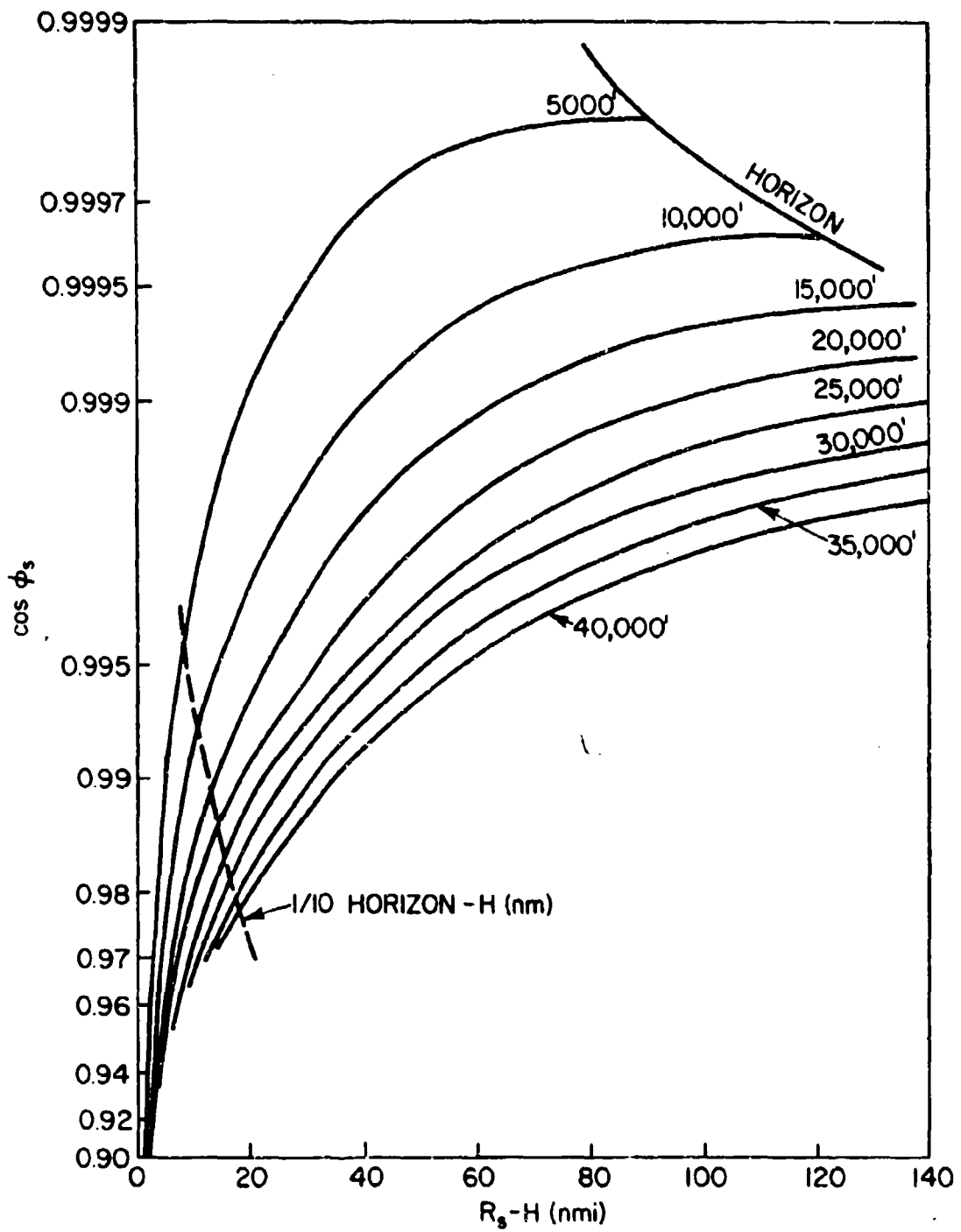


Fig. 3 - Elevation angle versus slant range

Equation 1) can be plotted simply by using Fig. 3 and offsetting the vertical axis to a point half-way between the selected maximum and minimum $\cos \theta_s$. This is done in Fig. 4 using,

$$R_{\max} = \text{Horizon} = (h^2 + 2rh)^{\frac{1}{2}}$$

$$R_{\min} = \text{Horizon}/10$$

Where: h = height of aircraft above surface

$$r = \frac{4}{3} \text{ radius of earth} \approx 4600 \text{ n mi.}$$

Effect of Error on MTI

To see the effect of this error on the succeeding processing, a model must be developed for the processing. Using the MTI processor to evaluate this error, the MTI improvement factor is defined as the input signal-to-clutter power to the output signal-to-clutter power. The MTI improvement factor, I_n , is given in Refs. 4 and 5 and is derived in appendix A for an n-stage MTI.

From Appendix A,

$$I_n = \frac{2^n}{n!} \left(\frac{f_r}{2\pi\sigma_c} \right)^{2n} \quad 2)$$

Where: f_r = pulse repetition frequency

σ_c = standard deviation of clutter spectrum.

Equation 2) is plotted in Fig. 5, n as a parameter.

The derivation of equation 2) assumed a zero-mean Gaussian clutter spectrum. But the TACCAR error represents a shift in the mean of the clutter spectrum by an amount, f_e . I_n is derived in Appendix B for this case and is given by:

$$I'_n = \frac{\frac{2^n}{n!} \left(\frac{f_r}{2\pi\sigma_c} \right)^{2n}}{L_n} = \frac{I_n}{L_n}$$

Where: L_n is the TACCAR loss which is given by

$$L_n = \frac{\left(\frac{f_e}{\sigma_c} \right)^{2n} + \sum_{k=1}^n \binom{2n}{2k} \left(\frac{f_e}{\sigma_c} \right)^{2n-2k} [1 \cdot 3 \cdot 5 \cdots (2k-1)]}{[1 \cdot 3 \cdot 5 \cdots (2n-1)]}$$

I'_n is shown in Figs. 6, 7, 8 for $n=1, 2, 3$ while L_n is shown in Fig. 9 for $n = 1, 2, 3$.

These curves show that the TACCAR loss can be significant, especially when the clutter spectral width, σ_c , is small. In this case, the MTI improvement factor is large resulting in good MTI performance. However, the TACCAR loss also gets large resulting in a considerable degradation in MTI performance. Conversely, it can be seen from these curves that when the variance of the clutter spectrum is large, then the estimate of the mean is not as critical to the MTI performance.

Figures 6, 7, and 8 show that the TACCAR loss will be appreciable for most airborne radar applications. The actual loss for a particular

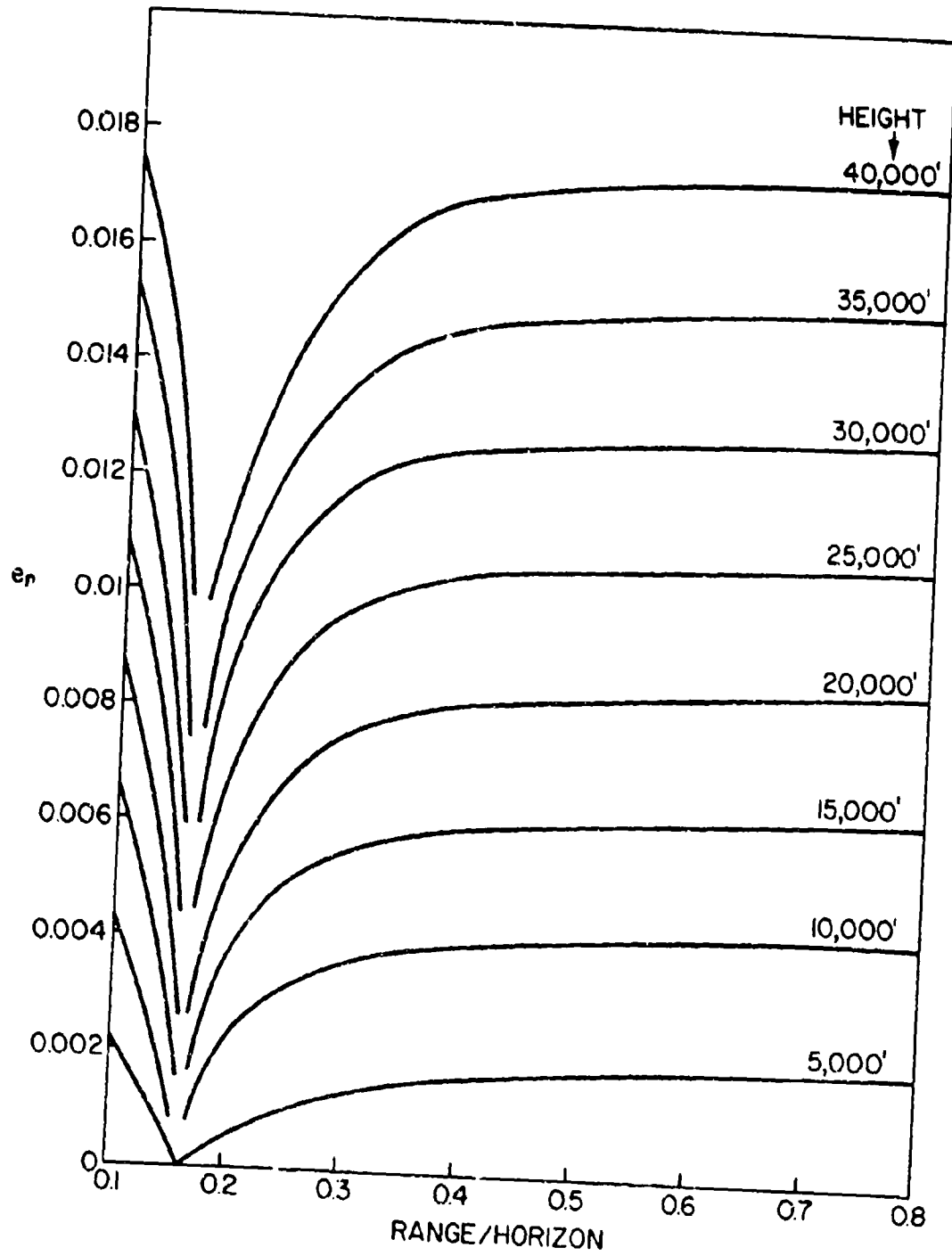


Fig. 4 - Normalized TACCAR error

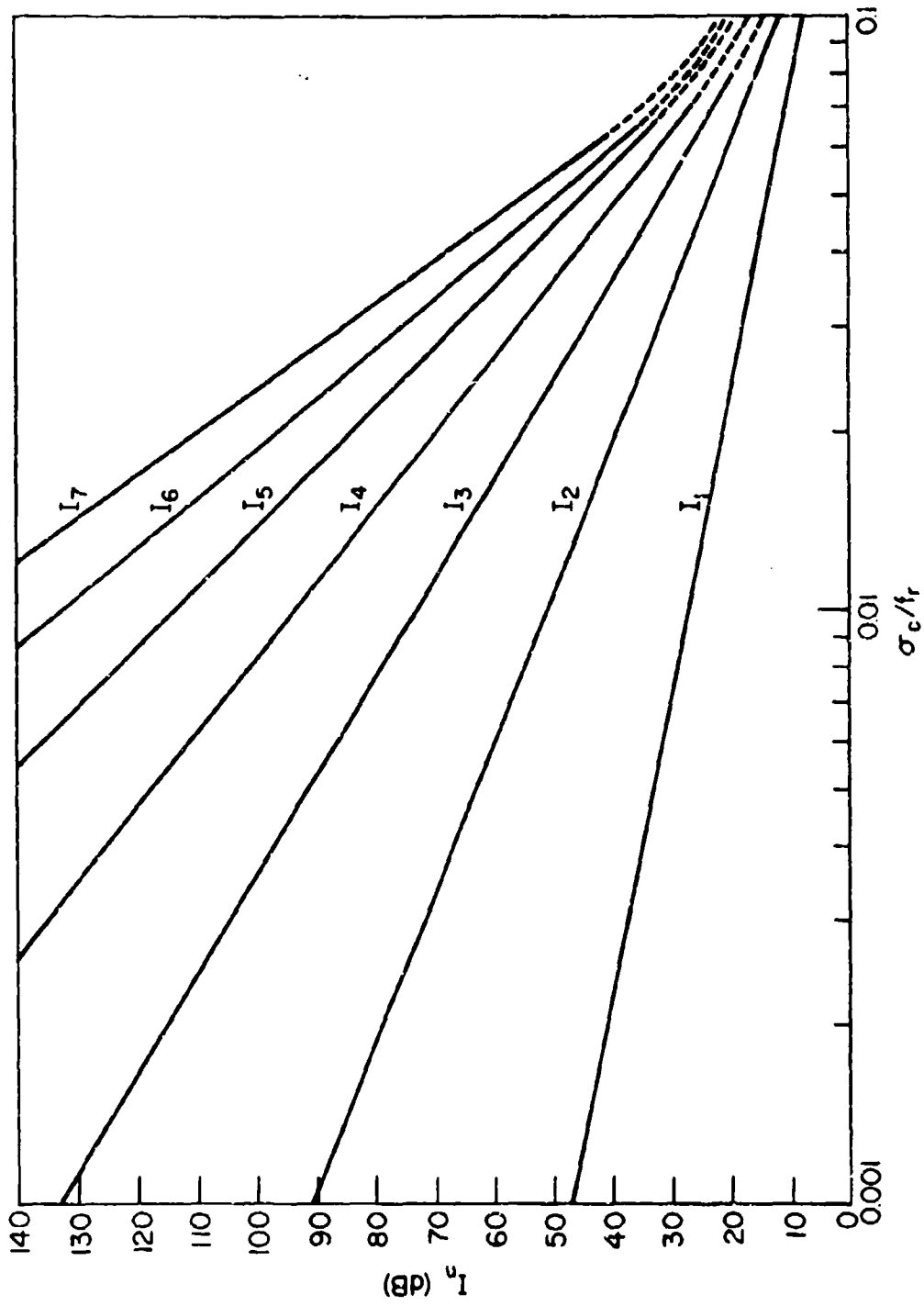


Fig. 5 - MTI improvement factor

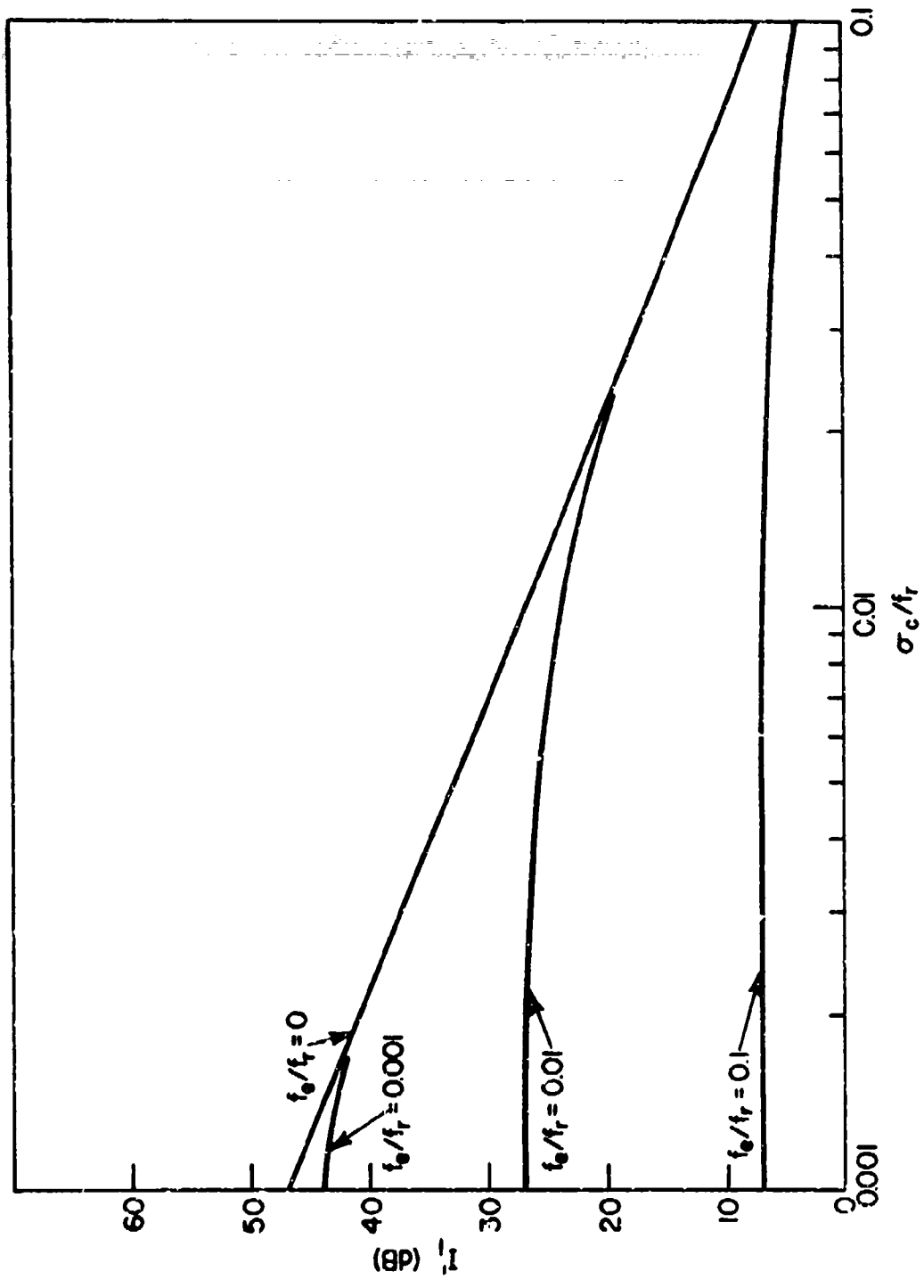


Fig. 6 - MTI improvement factor (single delay MTI)

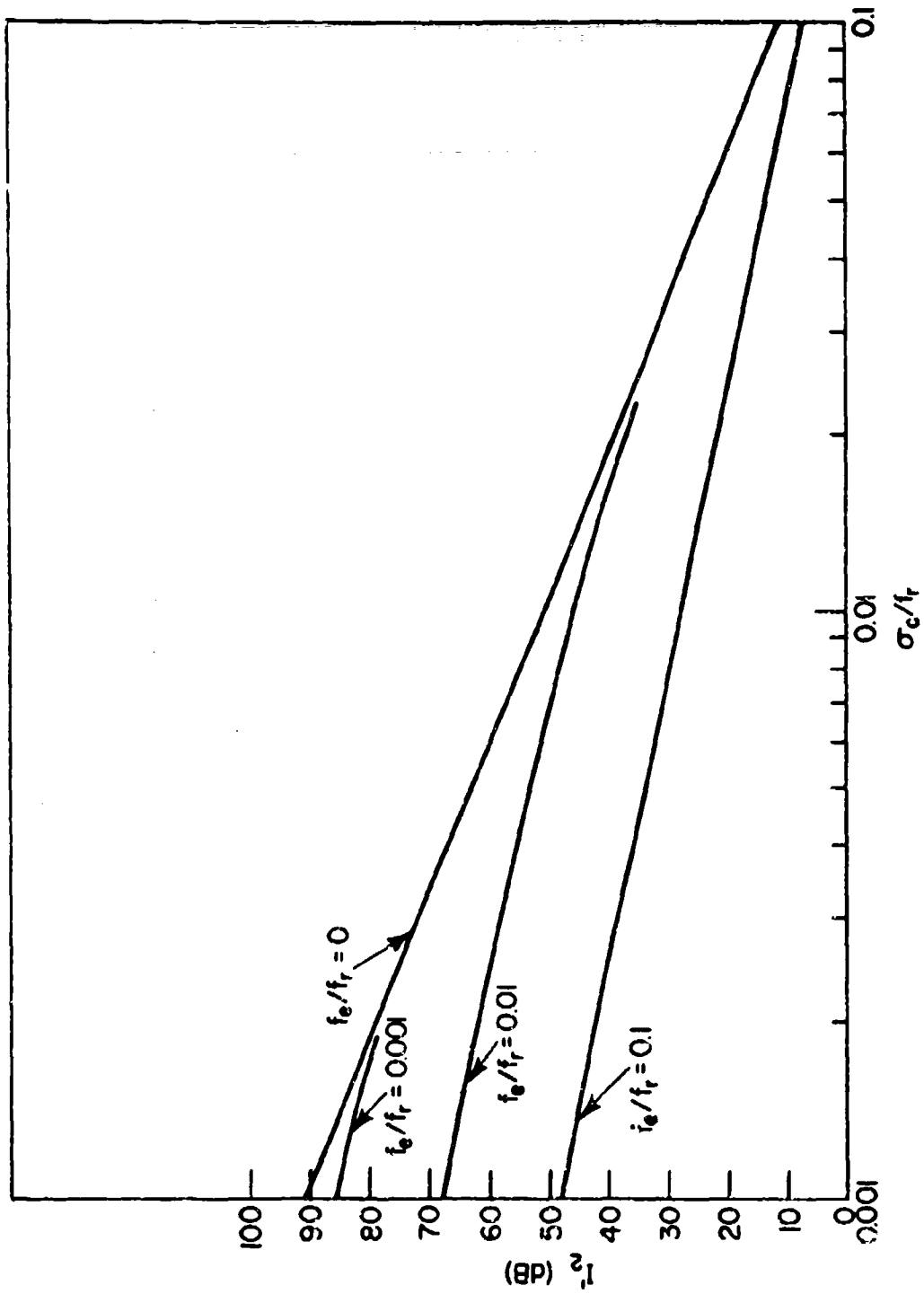


Fig. 7 - MTI improvement factor (double delay MTI)

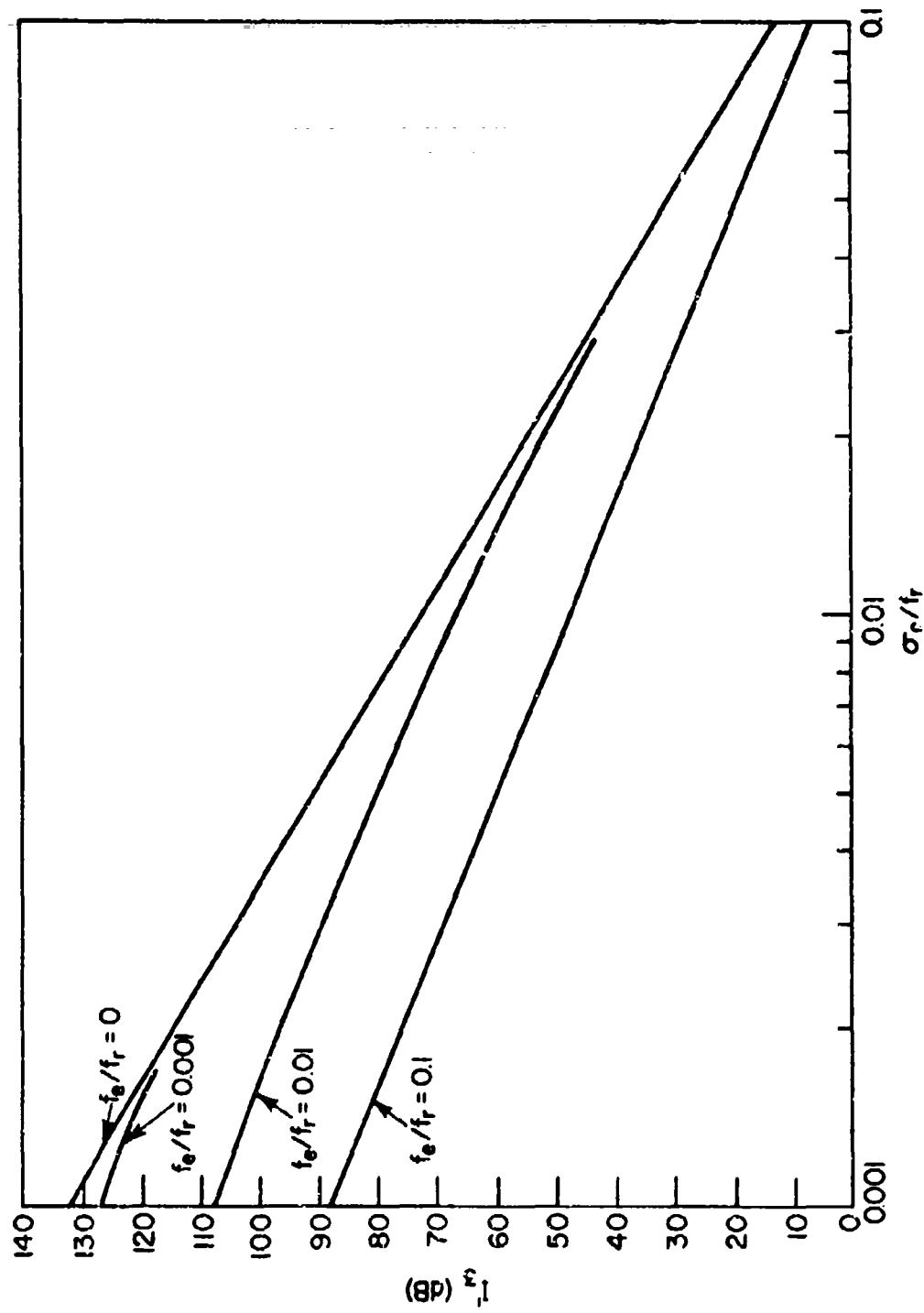


Fig. 8 - MTI improvement factor (triple delay MTI)

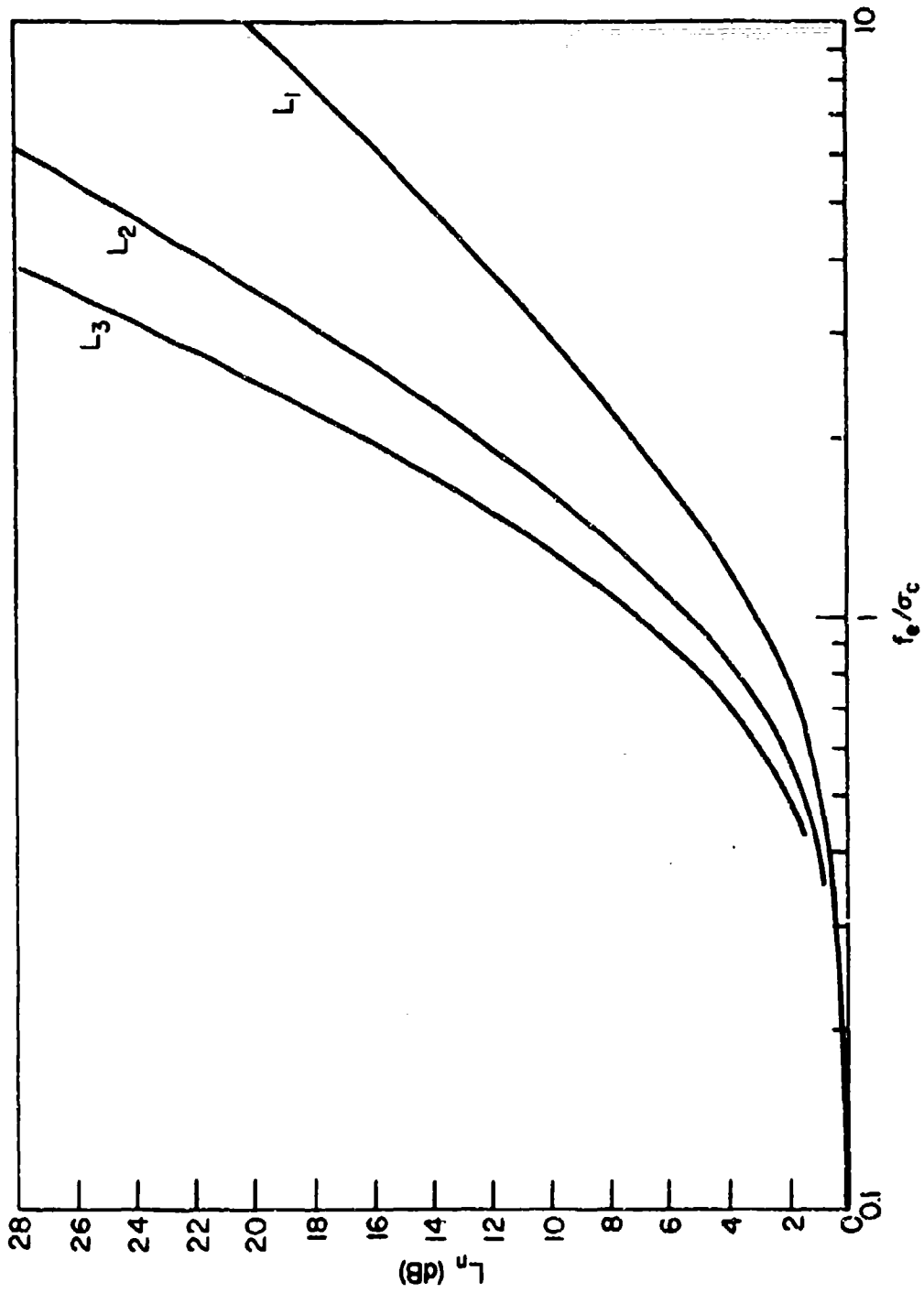


Fig. 9 - TACCAR losses

radar system can be obtained by using Fig. 5 for I_n and Fig. 9 for L_n . Then the resulting MTI improvement factor is,

$$I'_n \text{ (db)} = I_n \text{ (db)} - L_n \text{ (db)} .$$

Reduction of TACCAR Loss

TACCAR range error, the source of the TACCAR loss, can be essentially eliminated by making more than one correction with range. For a particular radar application, the magnitude of this TACCAR loss will determine if the additional complication is necessary.

The average doppler shift (i.e., the doppler shift on the axis of the beam) has been shown to be:

$$\bar{f}_d = \left(\frac{2v_p}{\lambda} \cos \theta_a \right) \cos \theta_s$$

Where: v_p = the platform velocity vector.

λ = transmitted wavelength.

θ_a = horizontal angle between v_p and axis of beam

θ_s = vertical angle between v_p and the incremental clutter patch under consideration.

The TACCAR range error resulted from estimating \bar{f}_d with:

$$\hat{f}_d = \left(\frac{2v_p}{\lambda} \cos \theta_a \right) \left(\frac{\cos \theta_{\max} + \cos \theta_{\min}}{2} \right)$$

which minimized the peak error. So that the TACCAR range error was defined as,

$$\begin{aligned} f_e &= \bar{f}_d - \hat{f}_d \\ &= \left(\frac{2v_p}{\lambda} \cos \theta_a \right) \left(\cos \theta_s - \frac{\cos \theta_{\max} + \cos \theta_{\min}}{2} \right). \end{aligned}$$

A normalized range error, e_n , was defined,

$$\begin{aligned} e_n &= \left| \frac{f_e}{\left(\frac{2v_p}{\lambda} \cos \theta_a \right)} \right| \\ &= \left| \cos \theta_s - \frac{\cos \theta_{\max} + \cos \theta_{\min}}{2} \right| \end{aligned}$$

and is shown in Fig.4.

From the mean doppler, \bar{f}_d , and the estimated mean doppler, \hat{f}_d , it is seen that the error results from the estimate of $\cos \theta_s$ by,

$$\widehat{\cos \theta_s} = \frac{\cos \theta_{\max} + \cos \theta_{\min}}{2}$$

This is illustrated by Fig. 10 (a). The peak of the normalized error is,

$$e_n^p = \frac{\cos \theta_{\max} - \cos \theta_{\min}}{2}$$

From Fig. 4, it can be seen that, to a good approximation, the peak error is constant with range because e_n is fairly constant over most of the range. The method of reducing TACCAR losses then becomes obvious, i.e., e_n^p may be reduced by correcting at more than one range.

Referring to Fig. 10a, the TACCAR loop is gated on during some interval including R_1 which results in an estimate of $\cos \theta_s$. This estimate is used for all ranges. If an additional TACCAR loop is added, then $\cos \theta_s$ can be estimated at two points, R_1 and R_2 , as shown in Fig. 10b. The estimate is switched from loop 1 to loop 2 at R_2 .

For two loops:

$$\widehat{\cos \theta_s} = \begin{cases} \frac{\cos \theta_{\max} + 3 \cos \theta_{\min}}{4} & , R < R_2 \\ \frac{3 \cos \theta_{\max} + \cos \theta_{\min}}{4} & , R > R_2 \end{cases}$$

If R_1 , R_2 , and R_3 are chosen to minimize e_n^p .

Then,

$$e_n^p = \frac{\cos \theta_{\max} - \cos \theta_{\min}}{4}$$

The peak error is reduced to one-half with the addition of the second loop.

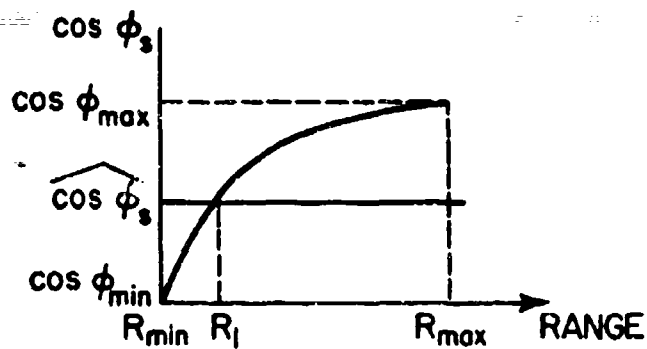
If a third loop is used (see Fig. 10c),

$$\widehat{\cos \theta_s} = \begin{cases} \frac{\cos \theta_{\max} + 5 \cos \theta_{\min}}{6} & , R < R_2 \\ \frac{\cos \theta_{\max} + \cos \theta_{\min}}{2} & , R_2 < R < R_4 \\ \frac{5 \cos \theta_{\max} + \cos \theta_{\min}}{6} & , R > R_4 \end{cases}$$

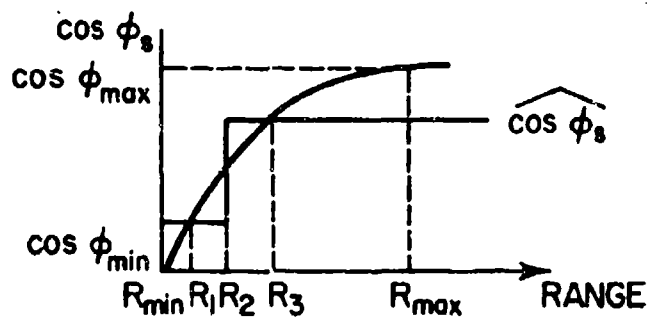
And,

$$e_n^p = \frac{\cos \theta_{\max} - \cos \theta_{\min}}{6}$$

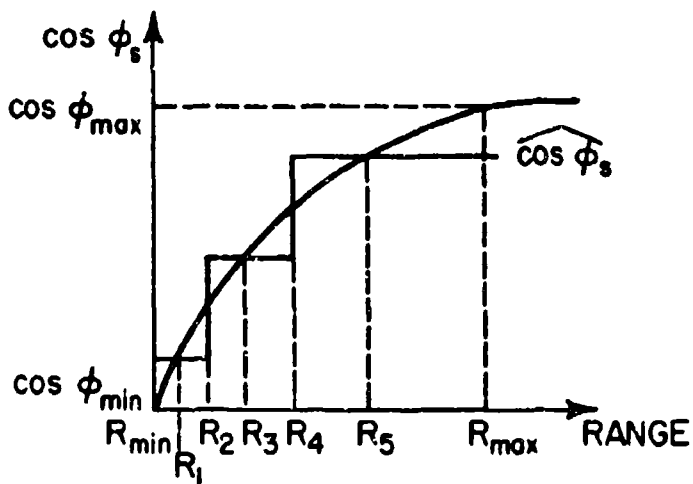
The peak error is reduced to one-third by the use of three loops.



(a)



(b)



(c)

Fig. 10 - 1, 2, 3 Point estimates of $\cos \phi_s$

With m loops,

$$\widehat{\cos \theta_s} = \begin{cases} \frac{\cos \theta_{\max} + (2m-1) \cos \theta_{\min}}{2m} & , R < R_2 \\ \frac{3 \cos \theta_{\max} + (2m-3) \cos \theta_{\min}}{2m} & , R_2 < R < R_4 \\ \vdots \\ \frac{(2m-1) \cos \theta_{\max} + \cos \theta_{\min}}{2m} & , R > R_{2m-2} \end{cases}$$

$$e_{1.}^P = \frac{\cos \theta_{\max} - \cos \theta_{\min}}{2m}$$

The peak error is reduced by $\frac{1}{m}$ with the use of m loops if the correction points $R_1, R_3, \dots, R_{2m-1}$ and the switching points $R_2, R_4, \dots, R_{2m-2}$ are selected to minimize e_R^P .

Fig. 4 can be used for an m -loop correction by replacing e_n by $m e_n$. Then Fig. 4 along with Fig. 9 can be used to determine the TACCAR loss for a particular radar application and for a particular number of correction points.

An implementation of additional corrections is shown in Fig. 11. A synchronizer is added which (1) generates gates of selected widths at the computed correction points and (2) generates switching signals to change the reference to the voltage-controlled oscillator at the computed switching points. Also, the necessary switching matrices and storage for m doppler estimates have been added. This implementation is equivalent to m parallel phase-lock loops. Each phase-lock loop can be optimized in the same way that previous TACCAR loops have been designed by putting a loop filter with each sample-and-hold circuit or alternatively by storing weighted sums of previous samples in each sample-and-hold circuit. The loop filters (or sample weights) are chosen for the desired loop performance.

Conclusions

The component of platform motion normal to the antenna aperture can cause significant losses to MTI performance. TACCAR corrects for the doppler caused by this component at one range interval. The operation of advanced MTI systems with higher MTI improvement factors and at higher transmitter frequencies require the TACCAR technique to be extended to make corrections at multiple range intervals. It has been shown that the reduction of the losses from this component of platform motion is limited only by the number of corrections.

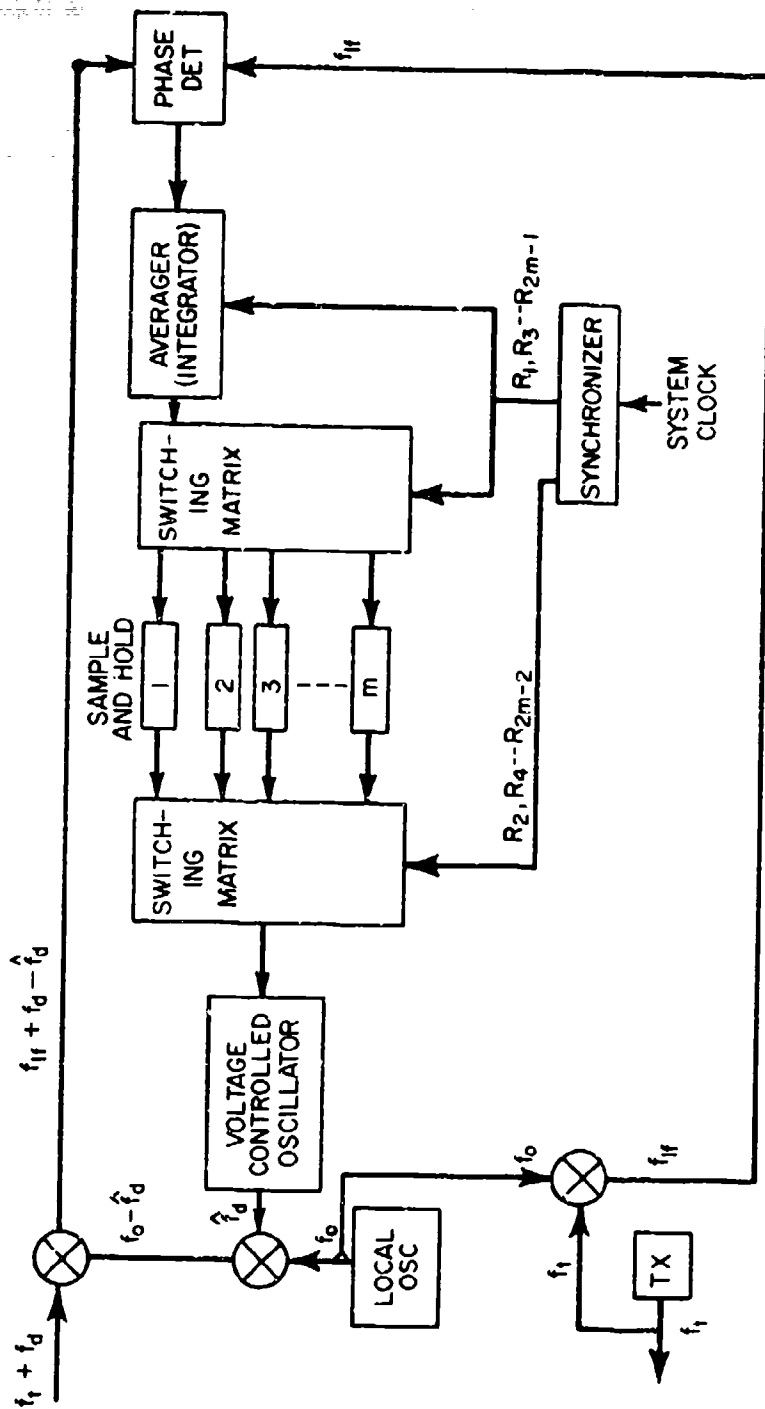


Fig. 11 - Simplified TACCAR with m correction points

A functional block diagram of a method of achieving this correction was shown in Fig. 11. Additional hardware is required to make additional corrections. By examining Fig. 4 (with e_n replaced by $m e_n$) and Fig. 9 for a particular application, it will be seen that as the number of corrections is increased each additional correction makes less and less improvement. Therefore, the additional hardware and the improvement for each correction will determine the number of corrections for a particular radar system. Also, methods of implementing these corrections with a minimum of additional hardware must be investigated.

There is a fundamental limitation in the number of correction intervals that can be used. For a large number of corrections, the correction interval may not contain enough samples to stabilize the loop. In this case additional samples would have to be taken on successive transmitted pulses. The result is a slower loop which may not be able to follow the change in doppler as the antenna is scanned. For most applications this limitation will not be reached since the number of corrections will be small and the loop response time must be greater than the transmitted pulse interval for good MTI action.

References

1. Skolnik, M. I., "Radar Handbook" McGraw-Hill, Inc., New York, 1970
2. Viterbi, A. J., "Principles of Coherent Communications", McGraw-Hill, Inc., New York, 1966
3. Gardner, F. M., "Phase Lock Techniques", John Wiley and Sons, Inc., New York
4. Barton, D. K., "Radar Systems Analysis", Prentice-Hall, Inc., Englewood Cliffs, N. J., 1964
5. Berkowitz, R. S., "Modern Radar", John Wiley and Sons, Inc., New York, 1965
6. Peirce, B. O., "A Short Table of Integrals," Ginn and Company, New York, 1929

APPENDIX A

Derivation of MTI Improvement Factor

Assume a Gaussian clutter spectrum,

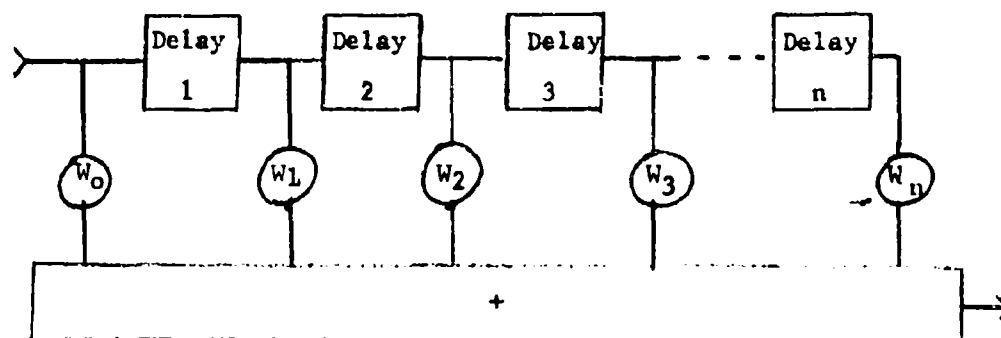
$$W(f) = W_0 \exp\left(-\frac{f^2}{2\sigma_c^2}\right)$$

The input clutter power is:

$$\begin{aligned} P_{1c} &= \int_{-\infty}^{\infty} W(f) df \\ &= W_0 \int_{-\infty}^{\infty} \exp\left(-\frac{f^2}{2\sigma_c^2}\right) df \\ &= \sqrt{2\pi} \sigma_c W_0 \end{aligned}$$

Assume binomial weights for the MTI shown in Fig. A1.

$$w_k = (-1)^k \binom{n}{k}, \quad k=0, 1, 2, \dots, n$$



n-stage MTI

Fig. A1

With binomial weights, the power gain of the MTI is given by:

$$G(f) = \left[2 \sin\left(\pi \frac{f}{f_r}\right) \right]^{2n}$$

Where

f_r = pulse repetition frequency

$$= \frac{1}{T}$$

T = delay of each delay line in Fig. A1.

The output clutter power is:

$$P_{oc} = \int_{-\infty}^{\infty} G(f) W(f) df$$

For successful MTI action, it must be assumed that the clutter spectrum is very much less than the pulse repetition frequency, i.e.: $\sigma_c \ll f_r$.

$$\begin{aligned} \text{Then: } P_{oc} &\approx \int_{-\infty}^{\infty} \left(2\pi \frac{f}{f_r}\right)^{2n} W_0 \exp\left(-\frac{f^2}{2\sigma_c^2}\right) df \\ &= W_0 \left(\frac{2\pi}{f_r}\right)^{2n} \int_{-\infty}^{\infty} f^{2n} \exp\left(-\frac{f^2}{2\sigma_c^2}\right) df \end{aligned}$$

This integral appears in most tables, for instance Ref. 6. Therefore,

$$P_{oc} = W_0 \left(\frac{2\pi}{f_r}\right)^{2n} [1 \cdot 3 \cdot 5 \cdots (2n-1)] \sqrt{2\pi} \sigma_c^{2n+1}$$

The square of the cancellation ratio is defined as

$$C^2 \triangleq \frac{P_{ic}}{P_{oc}} = \frac{\left(\frac{f_r}{2\pi\sigma_c}\right)^{2n}}{[1 \cdot 3 \cdot 5 \cdots (2n-1)]}$$

The average target gain is defined as the gain of the MTI for a target whose ambiguous doppler is uniformly probable of occurring anywhere between zero and f_r .

$$\begin{aligned} \bar{G} &\triangleq \frac{1}{f_r} \int_0^{f_r} G(f) df \\ &= \int_0^1 \left[2 \sin\left(\pi \frac{f}{f_r}\right)\right]^{2n} d\left(\frac{f}{f_r}\right) \\ &= \frac{2^{2n}}{\pi} \int_0^\pi \sin^{2n} \theta d\theta \end{aligned}$$

This integral is also found in Ref. 6.

$$\begin{aligned} \bar{G} &= \frac{2^{2n}}{\pi} \frac{[1 \cdot 3 \cdot 5 \cdots (2n-1)]}{2 \cdot 4 \cdot 6 \cdots 2n} \pi \\ &= \frac{2^{2n} [1 \cdot 3 \cdot 5 \cdots (2n-1)]}{2^n n!} \\ &= \frac{2^n}{n!} [1 \cdot 3 \cdot 5 \cdots (2n-1)] \end{aligned}$$

The MTI Improvement Factor is defined as the ratio of the output signal-to-clutter power to the input signal-to-clutter power. Therefore, the MTI Improvement Factor can be written as:

$$\begin{aligned} I_n &= c^2 \bar{G} \\ &= \frac{2^n}{n!} \left(\frac{f_r}{2\pi \sigma_c} \right)^{2n} \end{aligned}$$

APPENDIX B

Derivation of MTI improvement factor for clutter with non-zero mean spectrum

Assume a Gaussian clutter spectrum,

$$W(f) = W_0 \exp \left[- \frac{(f - f_m)^2}{2 \sigma_c^2} \right]$$

The input clutter power is:

$$\begin{aligned} P_{ic} &= \int_{-\infty}^{\infty} W(f) df \\ &= W_0 \int_{-\infty}^{\infty} \exp \left[- \frac{1}{2} \left(\frac{f - f_m}{\sigma_c} \right)^2 \right] df \\ &= \sqrt{2\pi} W_0 \sigma_c \end{aligned}$$

Assuming binomial weights for the MTI (see Appendix A), the power gain of an n-stage MTI is

$$G(f) = \left[2 \sin \left(\pi \frac{f}{f_r} \right) \right]^{2n}$$

Where: f_r = the pulse repetition frequency.

The output clutter power is:

$$\begin{aligned} P_{oc} &= \int_{-\infty}^{\infty} G(f) W(f) df \\ &= \int_{-\infty}^{\infty} \left[2 \sin \left(\pi \frac{f}{f_r} \right) \right]^{2n} W_0 \exp \left[- \frac{1}{2} \left(\frac{f - f_m}{\sigma_c} \right)^2 \right] df \end{aligned}$$

For successful MTI action, it is necessary to let

$$\sigma_c \ll f_r$$

With this assumption,

$$\begin{aligned} P_{oc} &\approx \int_{-\infty}^{\infty} \left(2 \pi \frac{f}{f_r} \right)^{2n} W_0 \exp \left[- \frac{1}{2} \left(\frac{f - f_m}{\sigma_c} \right)^2 \right] df \\ &= \left(\frac{2\pi}{f_r} \right)^{2n} W_0 \int_{-\infty}^{\infty} f^{2n} \exp \left[- \frac{1}{2} \left(\frac{f - f_m}{\sigma_c} \right)^2 \right] df \end{aligned}$$

Let:

$$f - f_m = x$$

Which implies:

$$f = x + f_m$$

$$df = dx$$

$$f^{2n} = (x + f_m)^{2n} = \sum_{i=0}^{2n} \binom{2n}{i} f_m^{2n-i} x^i$$

Therefore:

$$\begin{aligned} P_{oc} &= W_0 \left(\frac{2\pi}{f_r} \right)^{2n} \int_{-\infty}^{\infty} (x + f_m)^{2n} \exp \left[-\frac{x^2}{2\sigma_c^2} \right] dx \\ &= W_0 \left(\frac{2\pi}{f_r} \right)^{2n} \sum_{i=0}^{2n} \binom{2n}{i} f_m^{2n-i} \int_{-\infty}^{\infty} x^i \exp \left[-\frac{x^2}{2\sigma_c^2} \right] dx \end{aligned}$$

For i odd, this integral is zero since the integrand is an odd function.

For i even,

$$i = 2k$$

$$i = 0, 1, 2, \dots, 2n$$

$$k = 0, 1, 2, \dots, n$$

Then,

$$P_{oc} = W_0 \left(\frac{2\pi}{f_r} \right)^{2n} \sum_{k=0}^n \binom{2n}{2k} f_m^{2n-2k} \int_{-\infty}^{\infty} x^{2k} \exp \left[-\frac{x^2}{2\sigma_c^2} \right] dx$$

For $k = 0$,

$$\int_{-\infty}^{\infty} \exp \left[-\frac{x^2}{2\sigma_c^2} \right] dx = \sqrt{2\pi} \sigma_c$$

Therefore,

$$P_{oc} = W_0 \left(\frac{2\pi}{f_r} \right)^{2n} \left\{ \sqrt{2\pi} \sigma_c f_m^{2n} + \sum_{k=1}^n \binom{2n}{2k} f_m^{2n-2k} \int_{-\infty}^{\infty} x^{2k} \exp \left[-\frac{x^2}{2\sigma_c^2} \right] dx \right\}$$

This integral is shown in Appendix A,

$$\begin{aligned} P_{oc} &= W_0 \sqrt{2\pi} \sigma_c \left(\frac{2\pi \sigma_c}{f_r} \right)^{2n} \left\{ \left(\frac{f_m}{\sigma_c} \right)^{2n} \right. \\ &\quad \left. + \sum_{k=1}^n \binom{2n}{2k} \left(\frac{f_m}{\sigma_c} \right)^{2n-2k} [1 \cdot 3 \cdot 5 \cdots (2k-1)] \right\} \end{aligned}$$

The square of the cancellation ratio is,

$$C^2 = \frac{P_{1c}}{P_{0c}} = \left(\frac{f_r}{2\pi\sigma_c} \right)^{2n} \left\{ \left(\frac{f_m}{\sigma_c} \right)^{2n} + \sum_{k=1}^n \binom{2n}{2k} \left(\frac{f_m}{\sigma_c} \right)^{2n-2k} [1 \cdot 3 \cdot 5 \cdots (2k-1)] \right\}^{-1}$$

As shown in Appendix A, the average target gain for an n-stage MTI is

$$\bar{G} = \frac{2^n}{n!} [1 \cdot 3 \cdot 5 \cdots (2n-1)]$$

The MTI Improvement Factor is defined as the ratio output signal-to-clutter power and the input signal-to-clutter power. Therefore, the MTI improvement factor is

$$I_n = C^2 \bar{G} = \frac{\frac{2^n}{n!} \left(\frac{f_r}{2\pi\sigma_c} \right)^{2n} [1 \cdot 3 \cdot 5 \cdots (2n-1)]}{\left(\frac{f_m}{\sigma_c} \right)^{2n} + \sum_{k=1}^n \binom{2n}{2k} \left(\frac{f_m}{\sigma_c} \right)^{2n-2k} [1 \cdot 3 \cdot 5 \cdots (2k-1)]}$$

Security Classification

DOCUMENT CONTROL DATA - R & D

(Security classification of title, body of abstract and indexing annotation must be entered when the overall report is classified)

1. ORIGINATING ACTIVITY (Corporate author) Naval Research Laboratory Washington, D.C. 20390		2a. REPORT SECURITY CLASSIFICATION UNCLASSIFIED	
		2b. GROUP ---	
3. REPORT TITLE AIRBORNE RADAR MOTION COMPENSATION TECHNIQUES, EVALUATION OF TACCAR			
4. DESCRIPTIVE NOTES (Type of report and inclusive dates) An interim report on a continuing problem.			
5. AUTHOR(S) (First name, middle initial, last name) Grealie A. Andrews, Jr.			
6. REPORT DATE April 12, 1972	7a. TOTAL NO. OF PAGES 30	7b. NO. OF REFS 6	
8a. CONTRACT OR GRANT NO. NRL Problem 53R02-29	8b. ORIGINATOR'S REPORT NUMBER(S) NRL Report 7407		
8c. PROJECT NO. A360-5333/652B/2F00-141-601	8d. OTHER REPORT NO(S) (Any other numbers that may be assigned this report)		
10. DISTRIBUTION STATEMENT Distribution limited to U.S. Government Agencies only; test and evaluation, April 12, 1972. Other requests for this document must be referred to the Director, Naval Research Laboratory, Washington, D.C., 20390.			
11. SUPPLEMENTARY NOTES		12. SPONSORING MILITARY ACTIVITY Code 5333 Naval Air Systems Command	
13. ABSTRACT <p>Coherent signal processing in many classes of airborne radar systems is limited by the methods used to compensate for platform motion. Platform motion causes doppler shifts of returns which vary with the angle between the velocity vector and the scatterer. Because of the finite antenna beamwidth and finite transmitted plus length, the returns from many scatterers are received simultaneously. These returns have different doppler shifts which result in a spectrum of received doppler frequencies. This spectrum degrades the performance of radar systems that coherently process these returns.</p> <p>Time Average Clutter Coherent Airborne Radar (TACCAR) is a widely used technique to compensate for the component of motion which is parallel to the axis of the beam. This report evaluates TACCAR in terms of its improvement to moving target indicator (MTI) performance. It is shown that MTI performance can be improved significantly with extensions to the TACCAR concept.</p>			

DD FORM 1473 (PAGE 1)

S/N 0101-807-6801

Security Classification

14 KEY WORDS	LINK A		LINK B		LINK C	
	ROLE	WT	ROLE	WT	ROLE	WT
Airborne radar Radar platform motion Doppler processing Radar return signals Moving target indicator performance TACCAR (Time Average Clutter Coherent Airborne Radar)						

THIS REPORT HAS BEEN DELIMITED
AND CLEARED FOR PUBLIC RELEASE
UNDER DOD DIRECTIVE 5200.20 AND
NO RESTRICTIONS ARE IMPOSED UPON
ITS USE AND DISCLOSURE.

DISTRIBUTION STATEMENT A

APPROVED FOR PUBLIC RELEASE;
DISTRIBUTION UNLIMITED.